5. G. Servant *et al.*, *Science* **287**, 1037 (2000).
6. T. Jin, N. Zhang, Y. Long, C. A. Parent, P. N. Devreotes, *Science* **287**, 1034 (2000).
7. R. R. Neubig, M. P. Connolly, A. E. Remmers, *FEBS Lett.* **355**, 251 (1994).
8. R. Heim, R. Y. Tsien, *Curr. Biol.* **6**, 178 (1996).
9. The gene encoding the full-length YFP was fused to the NH_2-terminus of the Gβ gene. A Bgl II restriction site was added at the junction that consisted of two additional amino acids, arginine and serine. This β-YFP fusion protein was cloned into the CV5 vector. CV5 was derived from p88 by addition of an actin 15 expression cassette from pMC34 (*3*).
10. D. G. Lambright *et al.*, *Nature* **379**, 311 (1996).
11. M. A. Wall *et al.*, *Cell* **83**, 1047 (1995).
12. A. Kumagai *et al.*, *Cell* **57**, 265 (1989).
13. The gene encoding the full-length CFP was inserted into a Spe I site after residue 90, in the loop between the αA and the αB helices, of the Gα2 cDNA. The Spe I site also added a threonine and serine residue at the NH_2- and COOH-terminal boundaries of the insertion, respectively. This fusion was cloned into the CV5 vector. The $g\alpha2^-$ cells were transformed, and individual G418 resistant clones were selected. Rescued cells formed fruiting bodies and viable spores.
14. Equal amounts of plasmids carrying the Gα2-CFP and Gβ-YFP fusions were mixed and transformed into $g\alpha2^-$ cells. Individual G418 resistant clones were selected. Greater than 90% of transformed cells expressed both proteins.
15. The magnitude of the FRET fluorescence compared with that of Gβ-YFP directly excited at 490 nM and not relayed through Gα2-CFP varied from 7% (Fig. 2) to 12%. Emission spectra were collected between 460 and 600 nm (excitation at 440 nm) of the following lines: α2-CFP:β-YFP, a mixture of Gα2-CFP/$g\alpha2^-$ and Gβ-YFP/$g\beta^-$, and wild-type (AX3). Spectra were normalized to the fluorescence at 600 nm of the α2-CFP:β-YFP cells, and the wild-type spectrum was subtracted from the others. The corrected spectra were normalized to the fluorescence at 490 nm of the α2-CFP:β-YFP cells (see Fig. 2A). The amount of FRET fluorescence was determined by subtracting from the spectrum of the α2-CFP:β-YFP cells either the spectrum of the mixed cells or that of the Gα2-CFP/$g\alpha2^-$ cells. In the latter case, a further correction was made for the fluorescence emitted from Gβ-YFP/$g\beta^-$ directly excited at 440 nm.
16. C. Janetopoulos, P. N. Devreotes, unpublished data.
17. The residual signal may be due to cytoplasmic heterotrimer or a portion of membrane associated heterotrimer that remains during persistent stimulation.
18. The emission spectra of Gα2-CFP cells (excited at 440 nM), Gβ-YFP cells (excited at 440 or 490 nM), or mixtures of Gα2-CFP cells and Gβ-YFP cells (excited at 440 nM) did not change after stimulation.
19. R. L. Johnson *et al.*, *J. Biol. Chem.* **267**, 4600 (1992).
20. The EC_{50}'s of cAMP-induced actin polymerization, adenylyl cyclase activation, and calcium influx are 1 nM, 10 nM, and 200 nM, respectively. This suggests that there is a further amplification in the actin response and none in the adenylyl cyclase response. Interestingly, the calcium response requires more occupied receptors than does G-protein activation. This is consistent with the observation that the calcium response is partially independent of G-proteins.
21. L. J. Wu, P. N. Devreotes, *Biochem. Biophys. Res. Commun.* **179**, 1141 (1991).
22. S. van Es, P. N. Devreotes, *Cell Mol. Life Sci.* **55**, 1341 (1999).
23. C. A. Parent, P. N. Devreotes, *Annu. Rev. Biochem.* **65**, 411 (1996).
24. E. Snaar-Jagalska, S. van Es, F. Kesbeke, P. J. Van Haastert, *Eur. J. Biochem.* **195**, 715 (1991).
25. In another experiment, we added a single dose of 100 μM cAMP plus dithiothreitol to inhibit phosphodiesterase. Activation did not subside during 6 min of observation.
26. P. J. Lilly, P. N. Devreotes, *J. Cell Biol.* **129**, 1659 (1995).
27. R. A. Vaughan, P. N. Devreotes, *J. Biol. Chem.* **263**, 14538 (1988).
28. A. Mendez, N. V. Krasnoperova, J. Lem, J. Chen, *Methods Enzymol.* **316**, 167 (2000).
29. J. Chen, C. L. Makino, N. S. Peachey, D. A. Baylor, M. I. Simon, *Science* **267**, 374 (1995).
30. J. Vinós, K. Jalink, R. W. Hardy, S. G. Britt, C. S. Zuker, *Science* **277**, 687 (1997).
31. R. R. Gainetdinov *et al.*, *Neuron* **24**, 1029 (1999).
32. M. Caterina, P. N. Devreotes, J. Borleis, D. Hereld, *J. Biol. Chem.* **270**, 8667 (1995).
33. L. De Vries, B. Zheng, T. Fischer, E. Elenko, M. G. Farquhar, *Annu. Rev. Pharmacol. Toxicol.* **40**, 235 (2000).
34. D. M. Berman, A. G. Gilman, *J. Biol. Chem.* **273**, 1269 (1998).
35. A. B. Cubitt, R. Heim, L. A. Woollenweber, *Methods Cell Biol.* **58**, 19 (1999).
36. Enhanced CFP is a class 5 (F64L, S65T, Y66W, N146I, M153T, V163A) and the enhanced YFP is a class 4 (S65G, V68L, S72A, T203Y) GFP variant (*35*).
37. S. H. Zigmond, M. Joyce, J. Borleis, G. M. Bokoch, P. N. Devreotes, *J. Cell Biol.* **138**, 363 (1997).
38. Cells were scanned between 515 and 540 nm, normalized to the fluorescence at 527 nm of a 460- to 600-nm emission spectrum of α2-CFP:β-YFP cells (no cAMP). Spectra were corrected by subtraction of a normalized wild-type spectrum.
39. Spectra were first normalized to the integral from 475 to 550 nm. The spectrum at the highest dose was then subtracted from each of the other spectra. The areas under the differences curves were integrated from 475 to 520 nm and from 520 to 550 nm, and the absolute values were summed.

40. The authors wish to thank S. van Es, C. A. Parent, and L. Tang for advice and assistance in designing constructs and D. Murphy for help with the microscopy. Supported by NIH grants GM28007 and GM34933 to P.N.D. and an ACS Fellowship to C.J.

15 September 2000; accepted 12 February 2001

Length of the Flagellar Hook and the Capacity of the Type III Export Apparatus

Shigeru Makishima,[1] Kaoru Komoriya,[2] Shigeru Yamaguchi,[3] Shin-Ichi Aizawa[1]*

Length determination in biology generally uses molecular rulers. The hook, a part of the flagellum of motile bacteria, has an invariant length. Here, we examined hook length and found that it was determined not by molecular rulers but probably by the amount of subunit protein secreted by the flagellar export apparatus. The export apparatus shares common features with the type III virulence-factor secretion machinery and thus may be used more widely in length determination of structures other than flagella.

The bacterial flagellum, a rotary device for motility, is a supramolecular structure consisting of more than 20 different proteins that build up into three distinctive substructures: the filament, hook, and basal structure (*1, 2*). In *Salmonella enterica* serovar Typhimurium, the hook has an average length of 55 nm with a standard deviation of 6 nm (*3*), whereas the filament length varies over a wide range. In order to elucidate the mechanism regulating the invariant length of the hook, we used mutants that give rise to hooks of indefinite length, called "polyhooks." The mutation sites in these strains are not in the hook protein gene (*flgE*) but are in the *fliK* gene, suggesting that FliK acts as a length controller or a molecular ruler of the hook (*4–7*).

If FliK were a simple molecular ruler, truncated FliK's should produce shorter, not longer, hooks. However, all *fliK* mutants so far studied give rise to long polyhooks (*8*). In order to identify what controls the hook length, it is necessary to find mutants that produce short hooks. After an extensive survey, we found such strains with mutations in the *fliG*, *fliM*, and *fliN* genes.

Mutation in these three genes gives rise to different phenotypes, depending on the degree of their defects: Fla^- (filament-less) mutants derive from major defects, and Mot^- (motility-less) or Che^- (chemotaxis-less) mutants are from minor defects (*9, 10*). These three genes are commonly called the switch genes, putting an emphasis on the behavioral phenotype Che^-, in which the switch mechanism of the motor rotation is perturbed.

In the early stage of the survey by electron microscopy, we found short hooks in the intact flagella isolated from *fliG* mutants with Che^- phenotypes (Fig. 1A). The hook portion of the flagella looked less curved than that of the wild type, implying the shortness of the hook. In order to reveal the hook length more explicitly, hook-basal bodies (HBBs) were isolated (Fig. 1B), and the hook lengths were measured to produce diagrams of length distribution. The hook length of SJW2325 (*fliG*/Che^-) was 26.8 ± 8.0 nm, about half the length of the wild type (Fig. 2A).

Next, we isolated HBBs from both Che^- and Mot^- mutants of all the switch genes in our collection (three *fliG*/Che^-, seven *fliM*/Che^-, one *fliN*/Che^-, two *fliG*/Mot^-, five *fliM*/Mot^-,

[1]Department of Biosciences, Teikyo University, 1-1 Toyosatodai, Utsunomiya 320-8551, Japan. [2]Department of Applied Biochemistry, Utsunomiya University, Utsunomiya 321-8505, Japan. [3]Izumi Campus, Meiji University, 1-9-1 Eifuku, Suginami, Tokyo 168-0064, Japan.

*To whom correspondence should be addressed. E-mail: aizawa@nasu.bio.teikyo-u.ac.jp

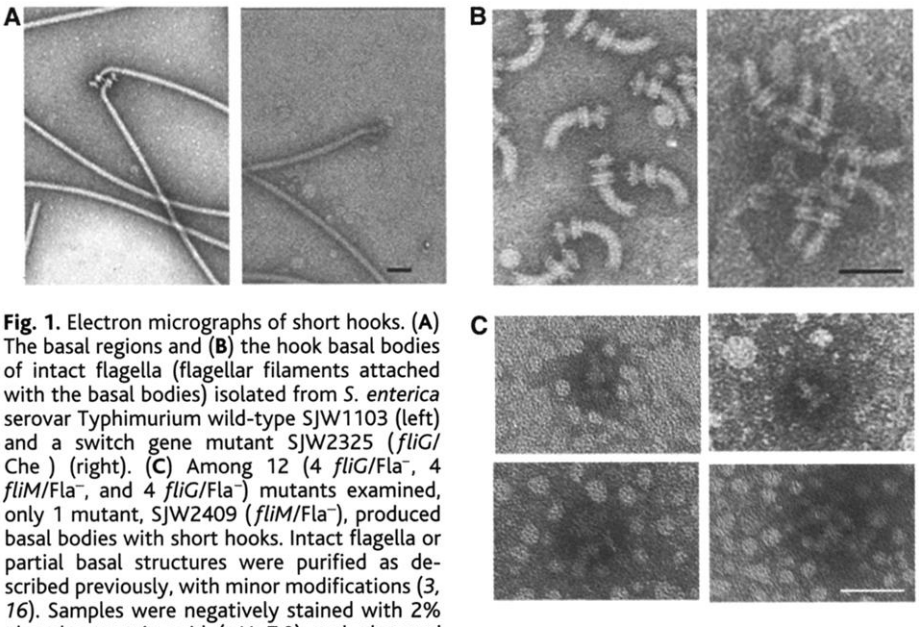

Fig. 1. Electron micrographs of short hooks. (**A**) The basal regions and (**B**) the hook basal bodies of intact flagella (flagellar filaments attached with the basal bodies) isolated from *S. enterica* serovar Typhimurium wild-type SJW1103 (left) and a switch gene mutant SJW2325 (*fliG*/Che) (right). (**C**) Among 12 (4 *fliG*/Fla$^-$, 4 *fliM*/Fla$^-$, and 4 *fliG*/Fla$^-$) mutants examined, only 1 mutant, SJW2409 (*fliM*/Fla$^-$), produced basal bodies with short hooks. Intact flagella or partial basal structures were purified as described previously, with minor modifications (*3, 16*). Samples were negatively stained with 2% phosphotungstic acid (pH 7.0) and observed with a JEM-1200EXII transmission electron microscope (JEOL, Tokyo). Micrographs were taken at an accelerating voltage of 80 kV. The scale bar represents 50 nm.

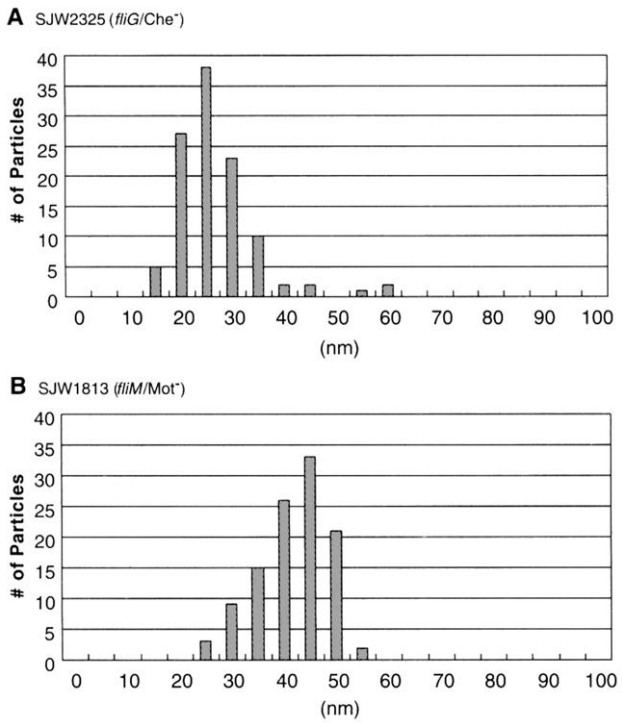

Fig. 2. Length distribution of hooks isolated from the switch gene mutants (**A**) SJW2325 (*fliG*/Che$^-$) and (**B**) SJW1813 (*fliM*/Mot$^-$). The hook length was measured directly from negatives (taken at a magnification of ×20,000) using a scale lupe (×15).

and four *fliN*/Mot$^-$ mutants). Their hook lengths were measured (Fig. 2 and Table 1). Many were as short as SJW2325, whereas the others were a little shorter than the wild type. For example, the hook length of SJW1813 (*fliM*/Mot$^-$) was 41.8 ± 6.8 nm, a length which is close to but distinguishable from wild-type hooks (Fig. 2B). All mutant hooks were shorter than the wild type and fell into one of two groups: 25-nm hook or 45-nm hook (Table 1).

Most of the Che$^-$ mutants examined gave rise to the 25-nm hook. The motor rotation of each Che$^-$ mutant is biased to either clockwise or counterclockwise, giving rise to tumbled or smooth swimming, respectively. Because both swimming patterns were observed in mutants with the 25-nm hook, we conclude that the shorter hook length does not affect the motor function or bias. Mot$^-$ mutants gave rise to both 25- and 45-nm hooks. Mot$^-$ mutations causing changes in the COOH-terminal half domain of each protein gave rise to 25-nm hooks, whereas those causing changes near the NH_2-terminal regions gave 45-nm hooks (Table 1).

The largest part of flagellum is constructed outside the cell, requiring an export system specific for the flagellar proteins. Most of the flagellar proteins have no leader sequences and are exported by a type III secretion system, the conventional name for one type of virulence-factor secretion systems in pathogenic bacteria (*11*). When the needle complex (NC) was identified as the type III secretion machinery (*12*), the morphological resemblance and homologous component proteins between HBB and NC suggested that these two structures share a common ancestor.

Needle length of *Salmonella*, which is invariant in wild type as found for hook length, can be elongated by an *invJ* (a *fliK* homolog) mutation (*13*). Furthermore, overproduction of MxiH (the needle protein) in *Shigella flexneri* also gives rise to polyneedles (*14*). Underlying these phenomena, we think, is the same mechanism as the hook length control. We now scrutinize the flagellar export apparatus to elucidate the mechanism.

The switch proteins form a hollow-cup structure called the C ring (C for cytoplasmic) beneath the flagellar basal body. A current model (*15*) for the C ring function emphasizes its roles in motor function; FliG forms the rotor, and a complex of FliM and FliN works in the switching of rotational direction. However, the C ring is involved in flagellar assembly before it works as a part of the motor; without switch proteins, the flagellum is not formed beyond the MS ring complex (*16*). The main body of the flagellar export apparatus is the C rod, which is located in the center of the C ring (*17*). How the C ring interacts with the C rod and how defects in the export apparatus affect the rotor or switch function at the same time are unknown. Because the C ring is a thin wall of proteins (*18, 19*), any conformational changes inside the ring would affect the whole structure.

We propose a model for the hook length control by the C ring. From the lattice constant of the hook, the number of hook subunits contained in the hook is calculated to be 11 subunits/5 nm, giving 121 subunits/55 nm for the wild-type hook, 99 subunits for the 45-nm hook, and 55 subunits for the 25-nm hook (*20*). Why should the lengths of short hooks be discontinuous? If this number of hook subunits was accumulated in the C ring at binding sites on the inner wall and the C ring was composed of ~30 identical units of the FliG, FliM, FliN complex, and if there were four binding sites on each unit of the C ring wall, the C ring would hold 120 hook subunits. If the binding sites decreased to three or two, the total number of the hook subunits would be 90 or 60, respectively. These numbers approximate to the numbers of hook subunits observed in the short mutant hooks. Thus, the physical capacity of the C ring may

Table 1. Hook length of switch gene mutants in *S. enterica* serovar Typhimurium. The phenotypes of Che$^-$ mutants were either tumbled (T) or smooth (S) swimming. The mutation sites were taken from (*25*) and (*26*); amino acid abbreviations are given in (*27*). The hook length data show the average hook length ± SD. The total number of measured particles is indicated in parentheses. n.d., not determined; dash indicates that only a few examples were observed (see Fig. 1C).

Gene	Phenotype	Strain number	Mutation sites	Hook length (nm)
fliG	Che$^-$ (T)	SJW2323	V135F	26.4 ± 6.9 (101)
	Che$^-$ (S)	SJW2325	V135L	26.8 ± 8.0 (110)
	Mot$^-$	SJW2834	R160H	44.0 ± 7.0 (110)
	Che$^-$ (T)	SJW2332	G185D	43.1 ± 8.7 (110)
	Mot$^-$	SJW2826	Δ282–287	28.5 ± 6.7 (111)
fliM	Che$^-$ (T)	SJW2308	E59K	24.1 ± 7.4 (70)
	Che$^-$ (T)	SJW2299	R60C	24.7 ± 6.4 (104)
	Che$^-$ (T)	SJW2309	R63C	25.9 ± 6.2 (71)
	Mot$^-$	SJW1813	H106P	41.8 ± 6.8 (109)
	Mot$^-$	SJW1764	F131C	45.7 ± 3.7 (109)
	Mot$^-$	SJW1806	G133D	45.1 ± 5.1 (114)
	Che$^-$ (S)	SJW2293	G143C	23.3 ± 6.0 (123)
	Mot$^-$	SJW1814	T147I	28.1 ± 7.6 (123)
	Che$^-$ (T)	SJW2312*	R181C	24.6 ± 7.3 (121)
	Che$^-$ (T)	SJW2311*	R181S	26.8 ± 6.7 (57)
	Che$^-$ (T)	SJW2310*	R181L	27.1 ± 8.4 (33)
	Mot$^-$	SJW1804	L250Q	26.5 ± 6.1 (110)
fliN	Che$^-$ (S)	SJW2287	G94S	23.4 ± 7.2 (62)
	Mot$^-$	SJW1765	L105Q	27.1 ± 7.0 (117)
	Mot$^-$	SJW1784	n.d.	47.0 ± 6.9 (148)
	Mot$^-$	SJW1809	n.d.	44.4 ± 6.3 (109)
	Mot$^-$	SJW1810	n.d.	46.2 ± 5.1 (93)
fliM	Fla$^-$	SJW2409	n.d.	—

*These mutants were derived from SJW806, whereas the others were from SJW1103 (*9*).

determine the hook length, and the C ring may act as a quantized measuring cup. The unit capacity and the subsequent unit hook length would be 30 subunits and 14 nm, as found in SJW2409 (*fliM* /Fla$^-$) (Fig. 1C).

If FliK is not a molecular ruler of hook length, then what is the role of FliK? The length distribution of polyhooks shows a peak at 55 nm, indicating that the hook length is controlled, even in the absence of FliK (*21*). In order to terminate the elongation, the hook-cap protein (FlgD) has to be replaced by a hook-filament junction protein (FlgK). However, FlgK itself is not necessary for the hook length control (*3*). In most *fliK* mutants, FlgD stays at the tip of the hook, allowing the continuous elongation of the hook (*22*). The flagellar secretion system has two modes: one specific for the hook proteins and the other for flagellin (*23*). These *flgK* mutants secrete large amounts of flagellin into media, indicating that the secretion mode is turned to the latter (*24*). Moreover, the *flgK* mutants secrete FliK, which terminates the secretion of hook proteins (*7*). Thus, FliK is likely to be required in the termination of hook elongation by changing the mode of secretion.

Thus, a mechanism of the hook length determination could be as follows. The hook monomers (FlgE) accumulate to fill the C ring and are secreted en bloc to form the hook of a finite length. When the C ring is empty, FliK is secreted, which converts the mode of secretion into that for flagellin. Then, FlgD at the tip of a nascent hook is replaced by FlgK, which terminates the hook elongation.

References and Notes

1. R. M. Macnab, in Escherichia coli *and* Salmonella typhimurium: *Cellular and Molecular Biology*, F. C. Neidhardt *et al.*, Eds. (American Society for Microbiology, Washington, DC, 1996), pp. 123–145.
2. S.-I. Aizawa, *Mol. Microbiol.* **19**, 1 (1996).
3. T. Hirano, S. Yamaguchi, K. Oosawa, S.-I. Aizawa, *J. Bacteriol.* **176**, 5439 (1994).
4. K. Kutsukake, *J. Bacteriol.* **179**, 1268 (1997).
5. K. Muramoto, S. Makishima, S.-I. Aizawa, R. M. Macnab, *J. Mol. Biol.* **277**, 871 (1998).
6. ———, *J. Bacteriol.* **181**, 5808 (1999).
7. T. Minamino, B. Gonzalez-Pedrajo, K. Yamaguchi, S.-I. Aizawa, R. M. Macnab, *Mol. Microbiol.* **34**, 295 (1999).
8. A. W. Williams *et al.*, *J. Bacteriol.* **178**, 2960 (1996).
9. S. Yamaguchi, H. Fujita, A. Ishihara, S.-I. Aizawa, R. M. Macnab, *J. Bacteriol.* **166**, 187 (1986).
10. S. Yamaguchi *et al.*, *J. Bacteriol.* **168**, 1172 (1986).
11. C. J. Hueck, *Microbiol. Mol. Biol. Rev.* **62**, 379 (1998).
12. T. Kubori *et al.*, *Science* **280**, 602 (1998).
13. T. Kubori, A. Aukhan, S.-I. Aizawa, J. E. Galan, *Proc. Natl. Acad. Sci. U.S.A.* **97**, 10225 (2000).
14. K. Tamano *et al.*, *EMBO J.* **19**, 3876 (2000).
15. S. A. Lloyd, F. G. Whitby, D. F. Blair, C. Hill, *Nature* **400**, 472 (1999).
16. T. Kubori, N. Shimamoto, S. Yamaguchi, K. Namba, S.-I. Aizawa, *J. Mol. Biol.* **226**, 433 (1992).
17. E. Katayama, T. Shiraishi, K. Oosawa, N. Baba, S.-I. Aizawa, *J. Mol. Biol.* **255**, 458 (1996).
18. I. H. Khan, T. S. Reese, S. Khan, *Proc. Natl. Acad. Sci. U.S.A.* **89**, 5956 (1992).
19. N. R. Francis, G. E. Sosinsky, D. Thomas, D. J. DeRosier, *J. Mol. Biol.* **235**, 1261 (1994).
20. C. J. Jones, R. M. Macnab, H. Okino, S.-I. Aizawa, *J. Mol. Biol.* **212**, 377 (1990).
21. S. Koroyasu, M. Yamazato, T. Hirano, S.-I. Aizawa, *Biophys. J.* **74**, 436 (1998).
22. K. Ohnishi *et al.*, *J. Bacteriol.* **176**, 2272 (1994).
23. T. Minamino, R. M. Macnab, *J. Bacteriol.* **181**, 1388 (1999).
24. K. Komoriya *et al.*, *Mol. Microbiol.* **34**, 767 (1999).
25. H. Sockett *et al.*, *J. Bacteriol.* **174**, 793 (1992).
26. V. M. Irikura *et al.*, *J. Bacteriol.* **175**, 802 (1993).
27. Single-letter abbreviations for the amino acid residues are as follows: C, Cys; D, Asp; E, Glu; F, Phe; G, Gly; H, His; I, Ile; K, Lys; L, Leu; P, Pro; Q, Gln; R, Arg; S, Ser; T, Thr; and V, Val.

28. We thank R. E. Sockett for polishing the English and T. Goto and S. Ishii for figures. This work was partially supported by Grant-in-Aid for Scientific Research (B) from The Ministry of Education, Science, Sports and Culture (Japan).

18 December 2000; accepted 6 February 2001
Published online 22 February 2001;
10.1126/science.1058366
Include this information when citing this paper.

Preferential Localization of Effector Memory Cells in Nonlymphoid Tissue

David Masopust, Vaiva Vezys, Amanda L. Marzo, Leo Lefrançois*

Many intracellular pathogens infect a broad range of host tissues, but the importance of T cells for immunity in these sites is unclear because most of our understanding of antimicrobial T cell responses comes from analyses of lymphoid tissue. Here, we show that in response to viral or bacterial infection, antigen-specific CD8 T cells migrated to nonlymphoid tissues and were present as long-lived memory cells. Strikingly, CD8 memory T cells isolated from nonlymphoid tissues exhibited effector levels of lytic activity directly ex vivo, in contrast to their splenic counterparts. These results point to the existence of a population of extralymphoid effector memory T cells poised for immediate response to infection.

After encounter with antigen, CD8 T cells differentiate into effector cells, which form a crucial arm of the adaptive immune response against intracellular pathogens through the action of cytokines and cell-mediated cytotoxicity (*1*, *2*). Activation leads to proliferation and a large increase in antigen-specific cytotoxic T lymphocytes (CTLs); this effector population contracts after resolution of the infection, leading to a stable memory popu-